Astronomy & Astrophysics manuscript no. output
November 10, 2021

Evolution of the ICRF stability from position time series analysis

N. Liu[1,2], S. B. Lambert[3], F. Arias[3], J.-C. Liu[1], and Z. Zhu[1]

[1] School of Astronomy and Space Science, Key Laboratory of Modern Astronomy and Astrophysics (Ministry of Education), Nanjing University, Nanjing 210023, P. R. China
e-mail: [niu.liu;zhuzi]@nju.edu.cn
[2] School of Earth Sciences and Engineering, Nanjing University, Nanjing 210023, P. R. China
[3] SYRTE, Observatoire de Paris, Université PSL, CNRS, Sorbonne Université, LNE, Paris, France
e-mail: sebastien.lambert@obspm.fr

Received; accepted

ABSTRACT

Context. The celestial reference frame is realized by absolute position of extragalactic sources which are assumed to be fixed in the space. The fixing of the axes is one of the crucial point for the International Celestial Reference System (ICRS) concept. However, due to various effects such as its intrinsic activity, the apparent position of the extragalactic sources may vary with time, resulting in a time-dependent deviation of the frame axes that are defined by positions of these sources.
Aims. We aim to evaluate the axis stability of the third realization of the International Celestial Reference Frame (ICRF3).
Methods. We first derive the extragalactic source position time series from observations of very long baseline interferometry (VLBI) at the dual S/X-band (2.3/8.4 GHz) between August 1979 and December 2020. We measured the stability of the ICRF3 axes in terms of the drift and scatter around the mean: (i) we estimate the global spin of the ICRF3 axes based on the apparent proper motion (slope of the position time series) of the ICRF3 defining sources; (ii) we also construct the yearly representations of the ICRF3 through annually averaged positions of the ICRF3 defining sources and estimate the dispersion in the axis orientation of these yearly frames.
Results. The global spin is no higher than 0.8 μas yr^{-1} for each ICRF3 axis with an uncertainty of 0.3 μas yr^{-1}, corresponding to an accumulated deformation smaller than 30 μas for the celestial frame axes during 1979.6–2021.0. The axis orientation of the yearly celestial frame becomes more stable as time elapses, with a standard deviation of 10–20 μas for each axis.
Conclusions. The axes of the ICRF3 are stable at about 10–20 μas among 1979.6–2021.0 and the axis stability does not degrade after the adoption of the ICRF3.

Key words. reference systems – astrometry – techniques: interferometric – quasars: general – catalogs

1. Introduction

The celestial reference frame provides the basic position reference for the astronomy and geoscience. The current realization of the celestial reference frame as adopted by the International Astronomical Union in 2018 is the third realization of the International Celestial Reference Frame (ICRF3; Charlot et al. 2020). The ICRF3 is constructed by positions of more than 4000 extragalactic sources based on very long baseline interferometry (VLBI) observations made at the dual S/X-, K-, and dual X/Ka-band (2/8 GHz, 24 GHz, and 8/32 GHz) since 1979. With several improvements in the modelling, for example, the correction of the Galactic aberration effect due to the acceleration of the solar system barycenter (MacMillan et al. 2019), and more accumulated data, the best position precision achieved for individual sources in the ICRF3 catalog has reached a level of 30 microarcsecond (μas).

The extragalactic sources are used to construct the celestial reference frame because they are distant from us so that they appear more compact and stable (i.e., showing a negligible motion) than other objects like Galatic stars. However, the apparent position of the extragalactic source varies with time, both in the radio and optical domain (e.g., see Andrei et al. 2009; Lambert 2013). This kind of position variability of extragalatic sources, also referred to as the astrometric instability, would lead to variations in the direction of the celestial frame axes defined by positions of those sources. This phenomenon is known as the celestial frame instability (e.g., see Lambert et al. 2008), a common issue for all kinds of extragalatic celestial reference frame such as the ICRF3 and the *Gaia* celestial frame (*Gaia*-CRF; Gaia Collaboration et al. 2018). The VLBI celestial frame instability would introduce additional noises to the VLBI products such as the Earth orientation parameter (EOP); the implication would be more serious for the nutation series since so far the VLBI is the sole technique that can measure the nutation angle. Dehant et al. (2003) and Lambert et al. (2008) study the impact of the celestial frame instability on the estimate of the nutation terms from the VLBI observations and report an additional noise of 15 μas in the amplitude of 18.6-year nutation term. The variability of extragalatic source may also degrade the precision of VLBI-*Gaia* frame alignment (Taris et al. 2013, 2016, 2018; Liu et al. 2018). Therefore, it is necessary to assess and monitor the instability level of the celestial reference system, which is the main motivation of this work.

There are several possibilities that make radio source apparently unstable. The main origin is the temporal evolution of radio source structure due to intrinsic variability such as the ejection of new jet features, which could manifest itself as an apparent proper motion (Fomalont et al. 2011; Moór et al. 2011) or positional offset along the jet (Plank et al. 2016). Other causes include the difference of radio source position as "seen" by different VLBI network (Dehant et al. 2003) and the weak micro-

lensing effect (Sazhin et al. 1998; Larchenkova et al. 2017, 2020).

Several authors propose indicators to characterize the source astrometric stability. Statistics based on the source coordinate time series are often used, for example, slope and standard deviation (Feissel-Vernier 2003), Allan variance (Gattano et al. 2018). The ICRF Working Group uses a quantity that considers the coordinate variations (weighted root-mean-square, WRMS) and the reduced chi-square for right ascension and declination (Fey et al. 2015; Charlot et al. 2020). In addition, other authors construct indicators based on the interstellar scintillation around the source (Schaap et al. 2013) and flux density time series (light curve; Shabala et al. 2014), which are found to correlate with the astrometric stability. Based on these indicators, sources with an unstable position can be recognized and ruled out, leaving only stable sources to define and maintain the axes of the celestial reference frame, which is known as the defining source (Feissel-Vernier 2003; Feissel-Vernier et al. 2006; Lambert & Gontier 2009). The stability of the VLBI celestial reference frame can be thus improved when a proper ensemble of stable sources are used as the defining source subset (Arias & Bouquillon 2004; Liu et al. 2017). A list of 303 sources with good astrometric behaviors known as the so-called ICRF3 defining sources was carefully selected, whose positions implicitly defines the axes of the ICRF3 (Charlot et al. 2020).

The ICRF axes are found to be stable on a level of 20 μas (Ma et al. 1998), which is further improved to 10 μas for the ICRF2 (Fey et al. 2015). These results are based on comparing the relative orientation of various subsets of sources. Adopting a different method, Lambert (2013) finds that the axis stability of the ICRF2 does not degrade after 2009, which is around 20 μas for each axis. Later, Lambert (2014) compares VLBI radio source catalogs submitted from different analysis centers of the International VLBI Service for Geodesy and Astrometry (IVS; Nothnagel et al. 2017) and reports an agreement of several tens of μas among these catalogs. Recently, Gattano et al. (2018) study the astrometric stability of extragalactic sources in the light of the Allan standard deviation of VLBI position time series. They conclude that the source position showing a stable behavior is likely to become unstable within a longer time span. It highlights the need of regularly monitoring the astrometric behaviors of extragalactic sources and the axis stability of the VLBI celestial reference frame, as already pointed out in Lambert (2013).

This work aims to assess the stability of ICRF3 axes based on the extragalactic source coordinate time series data, which have the advantage of being independent from VLBI global catalogs. Two methods were proposed for this purpose. One is to consider the accumulated effect due to the global spin of the VLBI celestial frame estimated from the apparent proper motion of extragalatic sources. The other one is to evaluate the variation of the axis orientation for yearly representations of the ICRF3.

2. Data and their preparation

The extragalactic source coordinate time series were derived from ten separate global solutions based on VLBI observations spanning from August 1979 to December 2020. The data consisted of about 16.3 M group delays made at dual S/X-band (2.4/8.3 GHz), in total 6974 sessions, which are publicly available at the IVS website[1]. We used the geodetic VLBI analysis software package Calc/Solve (version 20200123; Ma et al. 1986) to process these VLBI observations. The ten VLBI global solutions followed the same setup and parameterization, except some special configurations of radio source position estimate and celestial frame maintenance as explained in the following. In each solution, the position of one tenth of the sources (including one tenth of the defining sources) was degraded as sessions parameters. These ten groups of sources were chosen so that they distributed as uniformly as possible over the sky. The general technique description for these solutions can be found at the Paris Observatory Geodetic VLBI Center[2]; for the information about the special configurations, we refer to Lambert (2013) and Gattano & Charlot (2021). The root-mean-square of the postfit residual delay is about 40 picoseconds and the reduced χ^2 is 2.7.

We obtained the coordinate time series for 5290 extragalactic sources, among which 4543 sources are in common with the ICRF3 S/X-band catalogs, including all 303 ICRF3 defining sources. The median number of sessions in which a given were observed is 5 for all sources and it increases to 139 for the ICRF3 defining sources. The median value of mean observing epoch for individual sources is 2015.15 for the whole sample and 2013.11 for the ICRF3 defining source subset. The typical uncertainty (median value) in the coordinates for a given source is about 0.2 mas for the right ascension and 0.3 mas for the declination.

The axis stability of the celestial frames were evaluated in terms of the long-term drift and the wandering around the mean, as remarked below.

1. We estimated the apparent proper motions (slope) from coordinate time series and then fitted the global spin of the celestial reference frame based on these apparent proper motions. The spin multiplied by the time span during which the VLBI observations were made gives an estimate of the axis stability.
2. We constructed the yearly representations of the ICRF3 from the coordinate time series and compared the relative orientation of these yearly celestial reference frames with referred to the ICRF3 S/X-band catalog. The dispersion of the relative orientation angles provides another assessment of the axis stability.

The global (large-scale) features in any vector field on the celestial sphere can be described by the vector spherical harmonics (VSH; Mignard & Klioner 2012). Here we only considered the first degree of the VSH, which consists of a rotation vector $\boldsymbol{R} = (R_1, R_2, R_3)^{\mathrm{T}}$ and a glide vector $\boldsymbol{G} = (G_1, G_2, G_3)^{\mathrm{T}}$. The full equation can be expressed as

$$\begin{aligned} \Delta_{\alpha^*} = \; & -R_1 \cos\alpha \sin\delta - R_2 \sin\alpha \sin\delta + R_3 \cos\delta \\ & -G_1 \sin\alpha + G_2 \cos\alpha, \\ \Delta_{\delta} = \; & +R_1 \sin\alpha - R_2 \cos\alpha \\ & -G_1 \cos\alpha \sin\delta - G_2 \sin\alpha \sin\delta + G_3 \cos\delta. \end{aligned} \tag{1}$$

The notation $\alpha* = \alpha\cos\delta$ will be used throughout this paper. The rotation vector consists of rotation angles around the X-, Y-, and Z-axis and is used to characterize the stability of the ICRF3 axes.

Since we dealt with the rotation vectors both from the position offset and apparent proper motion field, different notations were used for clarity. Following the conventions used, for example, in Gaia Collaboration et al. (2018), we used the orientation offset vector $\boldsymbol{\epsilon} = (\epsilon_x, \epsilon_y, \epsilon_z)^{\mathrm{T}}$ to represent the rotation vector estimated from the position offset, meaning that $(\Delta_{\alpha^*}, \Delta_\delta)$ in Eq. (1) were substituted by $(\Delta\alpha^*, \Delta\delta)$. We denoted the rotation vector

[1] The data can be found at https://ivscc.gsfc.nasa.gov/products-data/data.html. A regular session is a collection of VLBI observations made within 24 hours. The full session list can be found at https://github.com/Niu-Liu/OpenFiles/blob/main/icrf3-axis-stability/nju2021s.arc.

[2] See http://ivsopar.obspm.fr/24h/opa2021a.eops.txt.

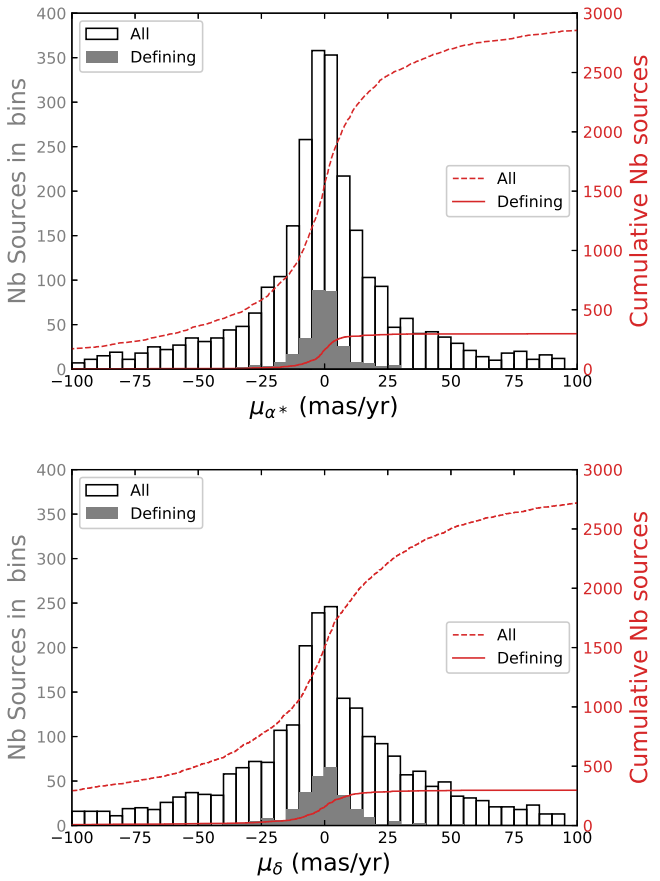

Fig. 1. Distribution of the apparent proper motion in the right ascension (*upper*) and declination (*lower*) for 3034 extragalctic sources fitted from their coordinate time series. The left and right vertical axes indicates the number of sources in the each bin and cumulative from the leftmost bin. The distribution for 299 sources among the so-called 303 ICRF3 defining source list were labelled in grey and red lines.

estimated from the apparent proper motion as $\boldsymbol{\omega} = (\omega_x, \omega_y, \omega_z)^{\mathrm{T}}$. This vector models the global spin of the celestial frame, that is, the change rate of the ICRF3 axis direction.

The rotation signal was estimated together with the glide parameters in the least-square fitting. The data were weighted by the full covariance matrix between right ascension and declination (i.e., including the covariace between the right ascension and declination). No outlier elimination was implemented in order to avoid the reduction of the rotation estimate caused by removing any source with a significant position offset or apparent proper motion in the elimination progress.

3. Analysis and results

3.1. Global spin from apparent proper motion

We estimated the apparent proper motion of the radio source based on their time series through a weighted least squares fitting. This model can be described as following.

$$\alpha\cos\delta = \mu_{\alpha*}(t-t_0) + \alpha_0\cos\delta,\ \ \delta = \mu_\delta(t-t_0) + \delta_0, \tag{2}$$

where $\mu_{\alpha*}$ and μ_δ are the apparent proper motion in the right ascension and declination, respectively, t_0 the mean epoch of the observing span for a given source.

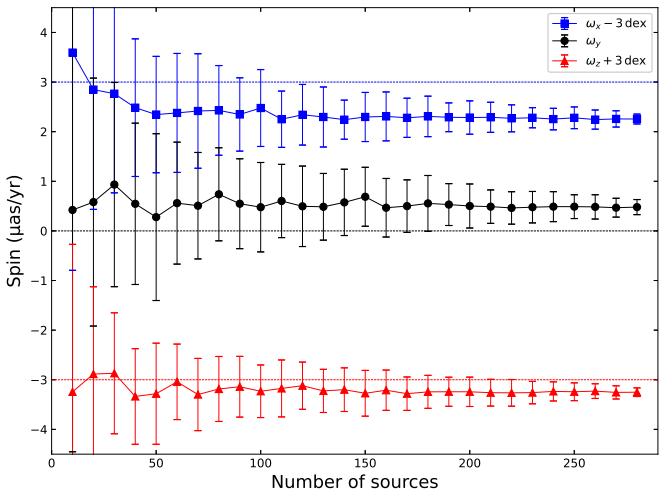

Fig. 2. Global spin estimated from the apparent proper motion versus the sample size used in the bootstrap sampling. The markers and errorbars stand for the mean value and standard deviation from 100 bootstrap samples, respectively.

All the data points were weighted by the inverse of the full covariance matrix for the right ascension and declination, which means that $\mu_{\alpha*}$ and μ_δ were fitted simultaneously. The data points whose distance to the mean position for a given source is greater than three times their formal errors in either right ascension or declination were considered as outliers and thus removed before estimating $\mu_{\alpha*}$ and μ_δ. Sources with less than five data points in the remaining time series were also removed from our list for the sake of a reliable proper motion determination.

We obtained the apparent proper motion for 3034 sources, 299 belonging to the ICRF3 defining source subset. Figure 1 depicts the distribution of the fitted proper motion. The median value of the apparent proper motion for all the sources is $-0.36\,\mu$as yr^{-1} in the right ascension and $0.26\,\mu$as yr^{-1} in the declination; they are $-0.57\,\mu$as yr^{-1} and $-0.33\,\mu$as yr^{-1} for the ICRF3 defining source subset. For more than half of sources in the whole sample, the apparent proper motion is within $\pm\,30\,\mu$as yr^{-1} both in the right ascension and declination.

We fitted the global spin from the apparent proper motion based on the 290 sources among the ICRF3 defining source list, and reported the result below.

$$\begin{aligned}\omega_x &= -0.73 \pm 0.27\,\mu\text{as yr}^{-1},\\ \omega_y &= +0.48 \pm 0.31\,\mu\text{as yr}^{-1},\\ \omega_z &= -0.25 \pm 0.21\,\mu\text{as yr}^{-1}.\end{aligned} \tag{3}$$

The total spin was estimated to be $\omega = 0.91 \pm 0.28\,\mu$as yr^{-1}, pointing to the direction of ($\alpha = 147^\circ \pm 20$, $\delta = -16^\circ \pm 14$).

We noted that the estimate from the least squares fitting might be biased by unreliable apparent proper motions of individual sources, and we also noted the fact that the uncertainty given by the least squares fitting is always underestimated. We used the bootstrap sampling technique to generate 1000 new samples (i.e., select 299 sources with replacement) and adopted the mean and standard deviation of the spin parameters derived these samples as a robust estimate of the unknowns and the associated formal uncertaintiy. The results are tabulated below.

$$\begin{aligned}\omega_x &= -0.71 \pm 0.42\,\mu\text{as yr}^{-1},\\ \omega_y &= +0.51 \pm 0.57\,\mu\text{as yr}^{-1},\\ \omega_z &= -0.24 \pm 0.36\,\mu\text{as yr}^{-1}.\end{aligned} \tag{4}$$

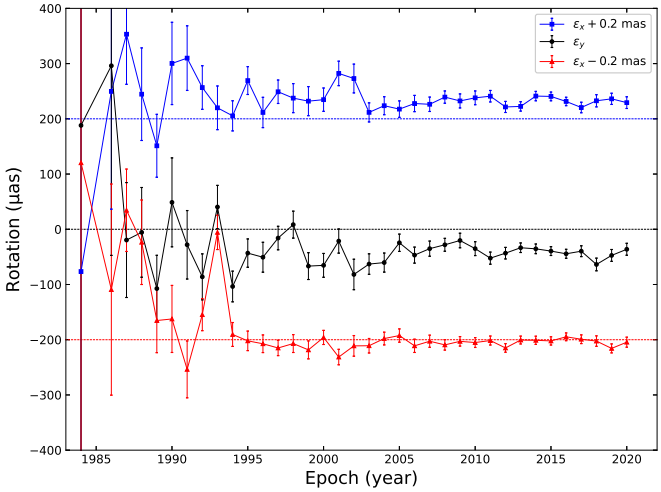

Fig. 3. Relative orientation of yearly celestial reference frames with respect to the ICRF3 S/X-band frame. The yearly celestial frames were constructed on the annual mean positions of the ICRF3 defining sources. The marker indicates the estimate of the orientation parameters while the bar shows the formal uncertainty from the least-squares fitting.

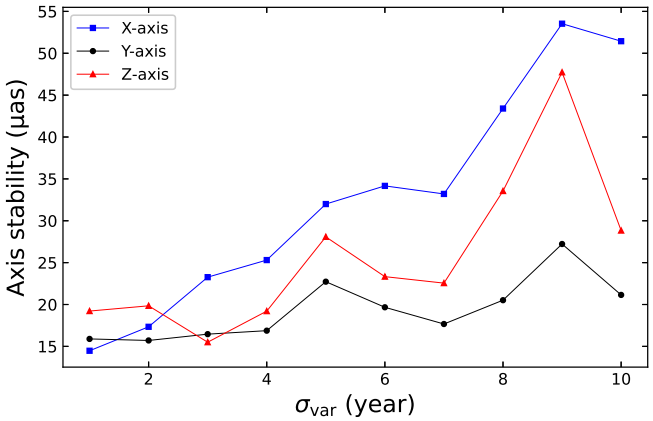

Fig. 4. Axis stability as a function of the amplitude of simulated positional drift.

One can easily find that the estimates in the Eqs. (3) and (4) are well consistent, but the bootstrap errors should be more realistic.

We wanted to know whether the axis stability of the celestial frame degrades when not all the ICRF3 defining sources are observed, as is the usual case for the VLBI campaigns. We randomly picked N sources from the sample (without replacement) and computed the rotation parameters. This procedure was repeated 100 times and we calculated the mean and standard deviation of the rotation parameters. The sample size N varies from 10 to 290, with a step of 10. Figure 2 presents the distribution of the mean spin (marker) and the standard deviation (errorbar) as a function of N. We found that the spin parameters were generally stable when $N \gtrsim 50$, where $\omega_{\rm x} \sim -0.60\,\mu{\rm as\,yr^{-1}}$, $\omega_{\rm y} \sim +0.53\,\mu{\rm as\,yr^{-1}}$, and $\omega_{\rm z} \sim -0.24\,\mu{\rm as\,yr^{-1}}$. The smaller errorbar at large values of N suggests that the estimate of the global spin converges when there is a sufficiently large number of the ICRF3 defining sources, no matter which sources are included.

We also repeated the procedures for all the sources with estimate of the apparent proper motion. The results agree well with those given in Eqs. (3)-(4) within the standard deviation.

The studies above suggests that only the spin around the X-axis is slight greater than the formal uncertainty from zero (c.f. Eq. (4)), therefore the spin in each axis of the ICRF3 cannot be considered as significant. Considering the time span of 41.4 yr long (1979.6–2021.0) and the subset of ICRF3 defining sources, the accumulated deformation is about 30 μas, 20 μas, and 10 μas for the X-, Y-, and Z-axis of the celestial reference frame, respectively. The uncertainty is about 20 μas considering the bootstrap errors (Eq. (4)) and about 10 μas using the least-square errors (Eq. (3)). As a result, a conservative estimation of the ICRF3 axis stability for this method is about 10–20 μas.

3.2. Orientation stability of yearly celestial reference frames

We averaged the source position weighted by their uncertainty from the coordinate time series within an one-year moving window with a step of also one-year (i.e., without overlaps) since 1979. An underlying (but may not always valid) assumption is that the characteristic time scale for a source to show a significant displacement is one year. The averaged source position of the ICRF3 defining sources within the same year window thus formed a yearly representation of the ICRF3. We only considered the yearly celestial frames with the number of the ICRF3 defining sources to be greater than six, which ruled out most yearly frames before 1986. By doing so, we formed 36 yearly celestial reference frames.

Figure 3 depicts the orientation offset angles of the yearly reference frame with respect to the ICRF3 S/X-band frame. The variation in the orientation offsets reduces significantly after 1995 and is further improved since 2002. The bumps during 2001–2002 in the ϵ_x is due to the unreliable position derived from little observations for some individual source (e.g., 1004-500). The weighted mean values of the orientation offset around the X-, Y-, and Z-axis are +32 μas, −24 μas, and +26 μas, respectively, while the corresponding WRMS with respect to the mean are about 13 μas, 16 μas, and 17 μas. When only considering the data points after 1995, the WRMS is reduced to 11 μas, 13 μas, and 7 μas for the X-, Y-, and Z-axis, respectively, whilst the corresponding mean values are changed to +33 μas, −41 μas, and −5 μas. Looking at data after 2018, we found that the scatters of the orientation for three ICRF3 axes are further reduced to 3 μas, 11 μas, and 6 μas, respectively.

Another method of constructing the yearly representation of the ICRF3 is to run a series of yearly VLBI global solutions with identical configuration but truncating the data collecting window (starting from 1979) to a certain year. The positions of the ICRF3 defining sources in each global solutions provides another yearly representation of the ICRF3. We tested this method and computed the deviation of the yearly celestial frame axes, which was fully consistent with what is presented in Fig. 3 within the formal error.

In short, the deviation of the yearly celestial reference frame axis is generally at the level of 10 – 20 μas. We did not detect significant degradation in the stability of the ICRF3 axes since 2018.

4. Discussion

As shown in the Eq. (4) and also Fig. 3, there is no statistically significant rotation in the ICRF3, which is very satisfactory. One question risen is that how much the axis stability would be changed by a very unstable defining source. To answer this ques-

tion, we simulated the behavior of the emitting center due to the variability of extragalatic source by a process with both Gaussian and Markovian characteristics as done in Bachchan et al. (2016). The position drift at time t_i was modeled as

$$\begin{bmatrix} \Delta\alpha_*(t_i) \\ \Delta\delta(t_i) \end{bmatrix} = \mathrm{e}^{-\Delta t_i/\tau_{\rm cor}} \begin{bmatrix} \Delta\alpha_*(t_{i-1}) \\ \Delta\delta(t_{i-1}) \end{bmatrix} + \begin{bmatrix} g_i^{\alpha_*} \\ g_i^{\delta} \end{bmatrix}, \quad (5)$$

where $\Delta t_i = t_i - t_{i-1}$ is the step length, $\tau_{\rm cor}$ the characteristic correlation timescale, and $g_i^{\alpha_*}$ and g_i^{δ} the Gaussian variable with zero mean and standard deviation

$$\sigma_i = \sigma_{\rm var}\sqrt{1-\exp(-2\Delta t_i/\tau_{\rm cor})}. \quad (6)$$

The amplitude of the positional variation $\sigma_{\rm var}$ ranged from 1 mas to 10 mas in the simulation. We considered source 0552+398 as the test source since it has the largest number of observing sessions. We assumed that $\tau_{\rm cor} = 5$ years. An example of the simulated position drift are given in Fig. A.1 in Appendix A. We considered the WRMS of the relative orientation of the yearly celestial frames (Sect. 3.2) as the indicator of the axis stability. Figure 4 depicts the relationship between these two quantities, from which we found a general increasing trend as expected. When $\sigma_{\rm var} \geq 3$ mas, the scatter of the X-axis orientation exceeds 20 μas, which means that the frame becomes more unstable than the actual level of 10–20 μas yr^{-1}. Figure A.2 presents the relative orientation of yearly celestial frames with respect to the ICRF3 when $\sigma_{\rm var} = 3$ mas. This simple simulation suggests a lower limit of 3 mas for the amplitude of source position variation when the orientation angle of the yearly frames may yield a detectable instability.

5. Conclusion

We evaluate the ICRF3 axis stability based on the coordinate time series of the extragalactic sources, which are derived from the geodetic VLBI observing program among 1979–2020. The main results are remarked below.

1. The global spin inferred from the apparent proper motion of the ICRF3 defining sources is no greater than 0.8 μas yr^{-1} for each axis with a formal error of 0.3 μas yr^{-1}, which corresponds to a directional deformation less than 30 μas for the ICRF3 axes accumulated in 1979–2020.
2. The scatter of the axis orientation for the yearly represents of the ICRF3 is on the order of 10–20 μas. There is no obvious degradation of stability for the ICRF3 axes after 2018 (i.e., the adoption of the ICRF3 as the fundamental reference frame).

Therefore, the ICRF3 axes are found to be stable at the level of 10–20 μas during August 1979 and December 2020.

In this work, the evaluation of the celestial frame axis stability is based on the source coordinate time series. This method catches both the mean variation of the axis orientation of the celestial frame and its time-dependent feature so that one can easily find and report the degradation of the axis stability if it occurs. Beside, this method is easy to launch and can provide the assessment of the axes stability regularly, making it a good alternative method for monitoring the celestial frame axis. Considering that the variability exists for most of extragalactic sources, we recommend regular assessments of the axis stability using the method based on the source coordinate time series.

Acknowledgements. N.L. and Z.Z. are supported by the National Natural Science Foundation of China (NSFC) under grant No. 11833004. N.L. is also supported by the Fundamental Research Funds for the Central Universities of China (grant No. 14380042) and China Postdoctoral Science Foundation (grant No. 2021M691530). This research had also made use of IPython (Perez & Granger 2007), Astropy[3] (Astropy Collaboration et al. 2018), the Python 2D plotting library Matplotlib (Hunter 2007), and NASA's Astrophysics Data System.

References

Andrei, A. H., Bouquillon, S., de Camargo, J. I. B., et al. 2009, in Journées Systémes de Référence Spatio-temporels 2008, ed. M. Soffel & N. Capitaine, 199–202
Arias, E. F. & Bouquillon, S. 2004, A&A, 422, 1105
Astropy Collaboration, Price-Whelan, A. M., Sipőcz, B. M., et al. 2018, AJ, 156, 123
Bachchan, R. K., Hobbs, D., & Lindegren, L. 2016, A&A, 589, A71
Charlot, P., Jacobs, C. S., Gordon, D., et al. 2020, A&A, 644, A159
Dehant, V., Feissel-Vernier, M., de Viron, O., et al. 2003, Journal of Geophysical Research (Solid Earth), 108, 2275
Feissel-Vernier, M. 2003, A&A, 403, 105
Feissel-Vernier, M., Ma, C., Gontier, A. M., & Barache, C. 2006, A&A, 452, 1107
Fey, A. L., Gordon, D., Jacobs, C. S., et al. 2015, AJ, 150, 58
Fomalont, E., Johnston, K., Fey, A., et al. 2011, AJ, 141, 91
Gaia Collaboration, Mignard, F., Klioner, S. A., et al. 2018, A&A, 616, A14
Gattano, C. & Charlot, P. 2021, A&A, 648, A125
Gattano, C., Lambert, S. B., & Le Bail, K. 2018, A&A, 618, A80
Hunter, J. D. 2007, Computing in Science and Engineering, 9, 90
Lambert, S. 2013, A&A, 553, A122
Lambert, S. 2014, A&A, 570, A108
Lambert, S. B., Dehant, V., & Gontier, A. M. 2008, A&A, 481, 535
Lambert, S. B. & Gontier, A. M. 2009, A&A, 493, 317
Larchenkova, T. I., Lutovinov, A. A., & Lyskova, N. S. 2017, ApJ, 835, 51
Larchenkova, T. I., Lyskova, N. S., Petrov, L., & Lutovinov, A. A. 2020, ApJ, 898, 51
Liu, J. C., Malkin, Z., & Zhu, Z. 2018, MNRAS, 474, 4477
Liu, N., Liu, J. C., & Zhu, Z. 2017, MNRAS, 466, 1567
Ma, C., Arias, E. F., Eubanks, T. M., et al. 1998, AJ, 116, 516
Ma, C., Clark, T. A., Ryan, J. W., et al. 1986, AJ, 92, 1020
MacMillan, D. S., Fey, A., Gipson, J. M., et al. 2019, A&A, 630, A93
Mignard, F. & Klioner, S. 2012, A&A, 547, A59
Moór, A., Frey, S., Lambert, S. B., Titov, O. A., & Bakos, J. 2011, AJ, 141, 178
Nothnagel, A., Artz, T., Behrend, D., & Malkin, Z. 2017, Journal of Geodesy, 91, 711
Perez, F. & Granger, B. E. 2007, Computing in Science and Engineering, 9, 21
Plank, L., Shabala, S. S., McCallum, J. N., et al. 2016, MNRAS, 455, 343
Sazhin, M. V., Zharov, V. E., Volynkin, A. V., & Kalinina, T. A. 1998, MNRAS, 300, 287
Schaap, R. G., Shabala, S. S., Ellingsen, S. P., Titov, O. A., & Lovell, J. E. J. 2013, MNRAS, 434, 585
Shabala, S. S., Rogers, J. G., McCallum, J. N., et al. 2014, Journal of Geodesy, 88, 575
Taris, F., Andrei, A., Klotz, A., et al. 2013, A&A, 552, A98
Taris, F., Andrei, A., Roland, J., et al. 2016, A&A, 587, A112
Taris, F., Damljanovic, G., Andrei, A., et al. 2018, A&A, 611, A52

[3] http://www.astropy.org

Appendix A: Simulation of positional variation for source 0552+398

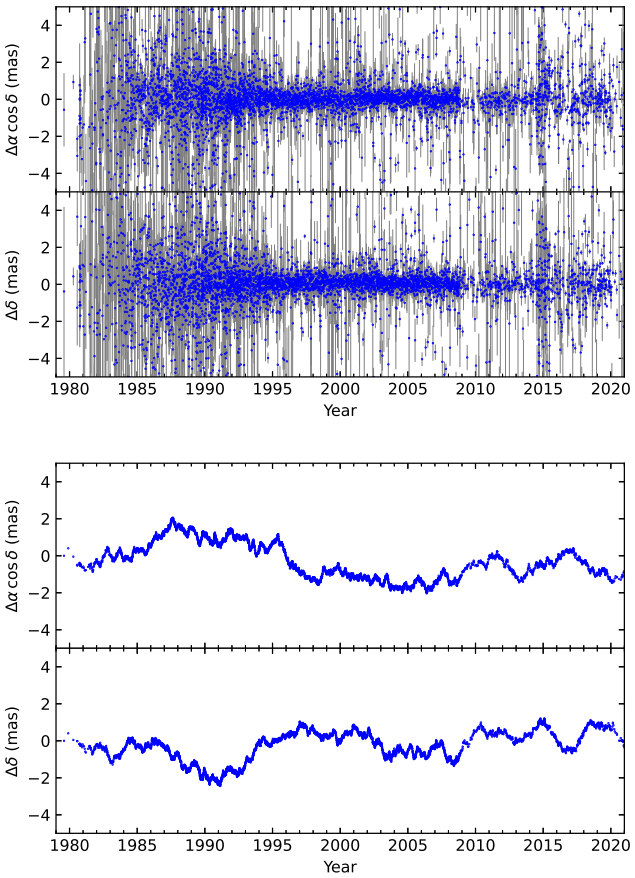

Fig. A.1. Top: the coordinate offset time series of source 0552+398 with referred to its position in the ICRF3 S/X-band catalog. Bottom: the simulated position drift due to the photometric variability. We assumed that $\tau_{\rm cor} = 5$ years and $\sigma_{\rm var} = 3$ mas.

Figure A.1 presents the coordinate time series of 0552+398 derived from the VLBI observations (top) and also simulated using Eq. 5 (bottom). If the simulated time series replace the real ones, the stability of the axis orientation of the yearly celestial frames would become worse, as shown in Fig. A.2.

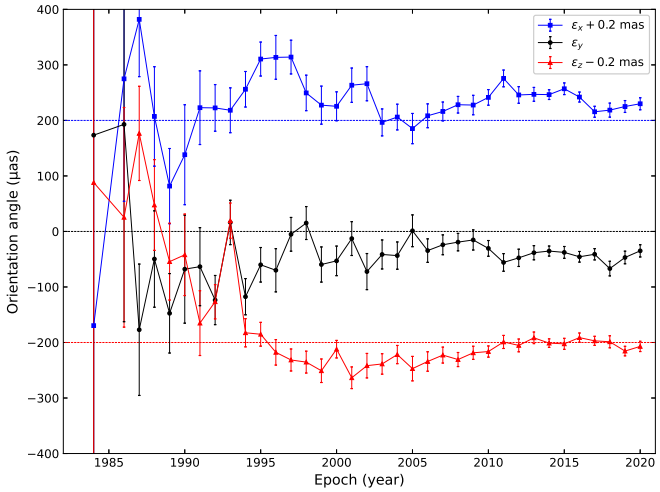

Fig. A.2. Relative orientation of yearly celestial reference frames with respect to the ICRF3 S/X-band frame in the case that source 0552+398 shows a position drift with an amplitude of 3 mas.